RESEARCH

Check for updates

Register of Dry Stone Domes. Simplified Method for Point Clouds

Cèlia Mallafrè Balsells[1] · Josep Maria López Besora[2] · Agustí Costa Jover[1] · Sergio Coll Pla[1]

Abstract

Dry-stone elements represent an important aspect of rural identity, and by nature, their constructive and volumetric elements have been eclipsed by their characteristics. Current massive data capture techniques, including photogrammetry, can offer new analysis procedures that will improve existing management and cataloguing methods. Such methods must address those characteristics that make it difficult to parametrize the formal features. This investigation focuses on a simplification of point clouds used to obtain formal and dimensional characteristics of specific elements. The management of the data obtained through a massive capture allows an analysis of elements both two- and three-dimensionally. The proposed procedure is tested in a dry-stone domed typology located in the north-eastern of the Iberian Peninsula.

Keywords Point cloud · Photogrammetry · Structure from motion · Dry stone

✉ Cèlia Mallafrè Balsells
    celia.mallafre@estudiants.urv.cat

    Josep Maria López Besora
    josep.m.lopez@urv.cat

    Agustí Costa Jover
    agusti.costa@urv.cat

    Sergio Coll Pla
    sergio.coll@urv.cat

[1] Reus School of Architecture (ETSA), Rovira i Virgili University (URV), Avinguda Universitat, 1, 43204 Reus, Spain

[2] Department of Computer Engineering and Mathematics, Rovira i Virgili University (URV), Carrer Marcellí Domingo, 1, 43007 Tarragona, Spain

Birkhäuser

Introduction

The aim of this study is to develop a method for parametrising different features from three-dimensional (3D) models. The original models are dry-stone buildings obtained through structure from motion photogrammetry (SFM). A methodology is then developed using a specific program to obtain the main features and post-process the point cloud.

Massive point capture data techniques are frequently used in cultural heritage studies (Pavlidis et al. 2007). Modelling and monitoring allow the analysis and protection of different heritage elements (Carnimeo et al. 2015; Foti et al. 2018). Such tools have many applications and are an important research topic (Barber et al. 2018). SFM is one of the most common techniques in this field owing to its ease of use and non-invasiveness (Guarnieri et al. 2004; Koutsoudis et al. 2014).

There are many examples of its application in various disciplines. This technology has been used in archaeology to facilitate the reading of damaged inscriptions (Andreu and Serrano 2019), to study pictures on rock walls (Jalandoni et al. 2018), and in the 3D modelling and seismic analysis of archaeological sites (Forlin et al. 2018). From an architectural perspective, photogrammetry is used to determine structural damage through a service analysis (Galantucci and Fatiguso 2019). In recent studies, the elements and geometric resolution of point clouds have been evaluated both manually and automatically (Fryskowska and Stachelek 2018).

Studies have also been conducted on the vernacular architecture of dry-stone structures (Restuccia et al. 2012; Rossi and Leserri 2013). In addition, photogrammetry has been used for tool registry and to enable the geometrical study of different constructions (Chen et al. 2017; Mineo et al. 2019). In this context, photogrammetry allows a fast rendering of 3D colorimetric features of the studied object and is a useful method for dry-stone buildings, which often have an irregular geometry with a complex access.

However, because the surfaces are extremely irregular, this method provides a noisy point cloud. Methods need to be applied to clean up the data for later studies of the area or volume. Along this line, studies have been conducted to standardise the point cloud along a building (Todisco et al. 2017) and remove noise (Vegas et al. 2010).

Dry-stone construction has been studied on the Iberian Peninsula since the beginning of the twelfth century (Rubió 1914; Torres 1933), although the main catalogues have only been published in recent years (García and Zaragozá 2000; Tarragó 2006). This building technique uses the leftover stone from farmlands and is conditioned by the culture, geography, and typology of the stone. There are, however, two common features: the use of a single material and stability based on equilibrium between elements under their own weight.

The method developed here has been tested on a basic dry-stone typology, i.e., an isolated construction with a circular floor plan, covered by a dome. This is a typical typology of which there are many examples around the world (Venerito et al. 2017; Mecca and Dipasquale 2009). The elements assessed in this study

are in the village of Tivenys (Tarragona, Spain). The surrounding area is rainfed land with fields of olives, almonds, and carob (Lluch and Giral 1967). Tivenys has a peculiar building typology, referred to as a '*cocó*' (pl. *cocons*). A *cocó* is composed of three elements: a rock-cut cavity; a dome to protect the structure from water, the sun, and animals and vegetation; and a water catchment surface (Fig. 1). The method developed here has been applied to a *cocó* dome, through which a point cloud can be used to study the main features of a building.

Methodology

The basic steps are data collection, data processing, and the development and application of a simplified point cloud formation process to obtain a mesh. Finally, some dimensional features are parameterised. The aim of the data collection is to obtain a point cloud by means of SFM. A total of 10 cocons were surveyed using a Nikon D7000 camera equipped with a Tamron LD XR DI AF 17–50 mm lens. To establish a coordinate system, a 1.45 m marker was divided every 5 cm. In addition, after the coordinate system was established, an auto calibration system, Agisoft Photoscan, was used for the creation of the point clouds (Table 1).

The objective of data processing is to use the SFM software to obtain the point cloud of the inner face of each dome. In all cases, the dome is conditioned based on the position of the door, which generates an information void.

The photogrammetric data are processed through an Intel® Core (TM) i7-4770 CPU operating at 3.40 GHz on a Windows 10 system with 16 GB of RAM. An NVIDIA Quadro K620 graphics card was used, and Agisoft Photoscan v.1.2.6.2834 software was employed.

Lighting limitations and the small dimensions of the domes complicated the photography process. Data describing each object consisted of one set of 3D

Fig. 1 Exterior and interior views of *cocó* 4

Table 1 Main parameters of point clouds obtained using SFM

COCONS	Name	Zone	Number of photographs	Quality of link point clouds	Number of point clouds
Cocó 1	de José	Majons	28	Medium	1,120,931
Cocó 2	de Joaquin	Argila	39	Medium	3,322,307
Cocó 3	de la Manela	lo Seguerol	39	Medium	2,396,514
Cocó 4	del Moreno	lo Seguerol	29	Medium	3,477,150
Cocó 5	de Rogelio	la Murta	117	Medium	4,820,003
Cocó 6	de Falló (I)	la Murta	92	Medium	6,338,801
Cocó 7	de Falló (II)	la Murta	75	Medium	5,145,146
Cocó 8	de Maria de Tanaro	la Murta	73	Medium	6,460,689
Cocó 9	de Gasparet	la Murta	109	Medium	7,917,751
Cocó 10	del Chicarro	la Murta	64	Medium	5,040,074

points, $X_i = (x_i, y_i, z_i)$, in world coordinates. The number of points obtained for all cases ranged from 600,000 to 3,500,000. For each case, a 3D representation of the points showed the existence of two other main problems: considerable overall noise and areas where data are sparse or non-existent.

Our method is based on the generation of a surface model made of triangles of a homogeneous size, which appropriately describes the shape of each object (Fig. 2). We developed a Linux-based program to clean and optimise the point cloud and generate a mesh to analyse it.

From the obtained mesh, it is possible to parametrise the dimensional features of each dome. 3DReshaper software was used to automatically obtain the data.
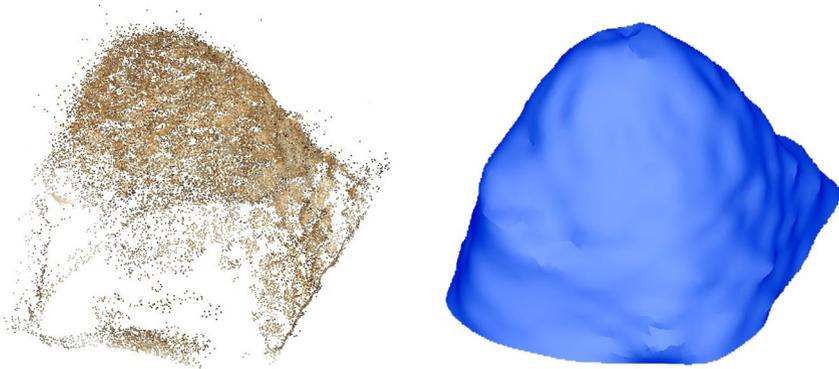
Fig. 2 Point cloud and mesh of a *cocó* dome

Theory and Calculation

Each cocó is described initially as a list of 3D points. The data are treated through several steps, allowing different values of the parameters to be tested (centre of the coordinates, number of slices, number of angular sections, and degree of Fourier approximation) until an appropriate representation is obtained. All necessary formulas and algorithms used (change in variables, sorting, Fourier expansion, and interpolation) are standard and implemented by the authors. The programs were written in FORTRAN and run in a Linux terminal environment. Together with the calculations, the programs also generate some scripts such that the calculations are conducted using the chosen parameter values, making it easier for the user to experiment with different sets of parameters. Meshes were obtained in STL ASCII format. The final treatment of the meshes obtained include a remeshing (conducted using Computational Geometry Algorithms Library (CGAL n.d.) routines) using 3DReshaper.

The mesh process from the point cloud entails three steps: computing the spherical coordinates and the data distribution, conducting a Fourier interpolation and approximation, and building the mesh, which are described in the following.

Step 1: Computing Spherical Coordinates and Data Distribution

First, we consider all points of one set and compute the geometric centre using the maximal and minimal values of z. We then choose a point of view, P_0, placed somewhere along a vertical line passing through the geometric centre (Fig. 3). As a general rule, point P_0 is chosen halfway between the top and bottom values of z,

Fig. 3 Example of two possible choices for prospective P_0. Green dots correspond to the projection along the *YZ* plane of all points from one set whose *x* coordinate is within 16 mm of the *x* coordinate of the centre. The red vertical line passes through the centre (not represented here). Blue points are two possible choices for the perspective. The two black angles represent two possible intervals within the θ domain, each for a different choice of perspective
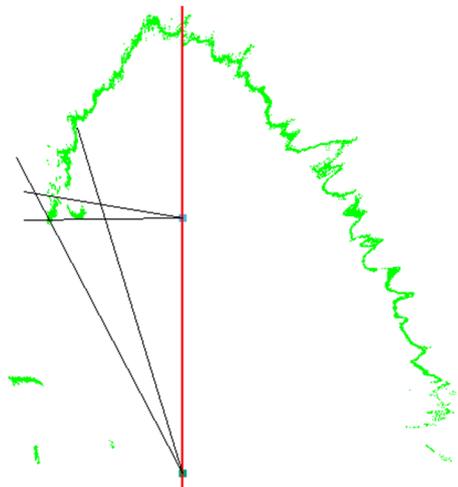
but some other position may be preferable in some cases depending on the specific characteristics of the particular object (e.g., notoriously bulky structures or doors).

Next, spherical coordinates with respect to a reference with centre P_0 are computed for all points of X_i, that is, r_i, θ_i, φ_i, where $r_i = d(P_0, X_i)$, and θ_I and φ_i correspond to the polar and azimuthal angles, respectively; note that $\theta = 90°$ from the geographic latitude, and φ corresponds to the geographic longitude. Then, the θ and φ domains are divided into intervals with representative values of θ_m, φ_k, where $m = 1,\ldots$, nSlices and $k = 1, \ldots,$ nAngles; this creates regions of nSlices × nAngles. Finally, for each region corresponding to m, k we consider all points whose values of θ_i, φ_i are in the corresponding mth and kth intervals; if the number of points reaches a given threshold, the median ρ_{mk} of the r_i values for these points is computed.

Step 2: Performing a Fourier Interpolation and Approximation

For a given region, the median ρ_{mk} provides a robust estimator of the central values for r_i within this region. However, a representation of all ρ_{mk} values shows that some of them can also be considered outliers when compared to the rest. This noise introduces a major problem in those regions that lack a ρ_{mk} value; in addition, in some cases, it can have an excessive effect on small-scale structures. To solve these problems and obtain a full and more averaged description of the shape, a Fourier analysis is conducted. For every fixed value of θ_m we consider the set of points φ_k, ρ_{mk} for $k = 1, \ldots,$ nAngles and compute the estimates of the missing values of ρ_{mk} through an interpolation (Fig. 4a). A Fourier expansion is then calculated to a suitable degree and used to obtain a new set of points φ_k, ρ_{mk} that describe a smoother fully closed curve (Fig. 4b–d).

Step 3: Mesh Building

From the results of step 2, we obtain a set of points in world coordinates, $X_{mk} = (x_{mk}, y_{mk}, z_{mk})$. Note that, for a fixed θ_m, the values for z_{mk} need not to be constant because the radius depends on the value of longitude φ_k.

Obtaining ring-shaped triangular meshes that join any two adjacent curves (given by m and $m+1$) is straightforward; it is done by defining the two triangles that split the rectangles with vertices X_{mk}, $X_{m,k+1}$, $X_{m+1,k}$, and $X_{m+1,k+1}$ (Fig. 5a). The full mesh is completed by adding all the ring-shaped triangular meshes together, with the addition of a spherical-cap shaped mesh made from the highest placed closed curve and the top point (Fig. 5b).

Even if at this stage we have a triangular mesh that is representative of the original set of points, it is convenient to conduct further calculations to replace this mesh with a new one which has the same overall geometry but with triangles that are more regular in shape and size. This is conducted using CGAL, which implements the incremental triangle-based isotropic remeshing algorithm introduced by Botsch et al. (2004: 185–192; Botsch et al. 2010) (Fig. 5c).
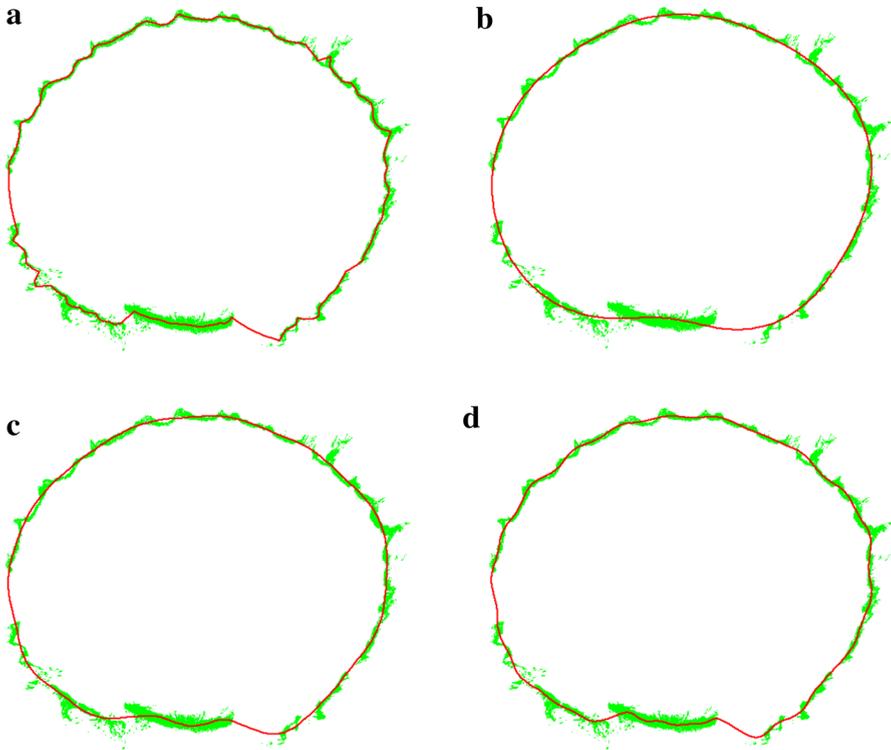
Fig. 4 **a** An example with *nSlices* = 50 and *nAngles* = 180. Green dots correspond to the projection on the XY plane of the 96,225 points for which $m=33$. The red line is the polygon defined by the 180 points in the Cartesian coordinates obtained from φ_k, ρ_{mk}, where $m=33$, and $k=1,\ldots$, 180 (see the text for the meaning of φ_k, ρ_{mk}). **b** An example with *nSlices* = 50 and *nAngles* = 180. Green dots correspond to the projection on the XY plane of the 96,225 points for which $m=33$. The red line is the polygon defined by the 180 points in the Cartesian coordinates obtained from φ_k, ρ_{mk}, where $m=33$ and $k=1,\ldots$, 180 (see the text for the meaning of φ_k, ρ_{mk}) in the case of a Fourier approximation on the order of 5. **c** An example with *nSlices* = 50 and *nAngles* = 180. Green dots correspond to the projection on the XY plane of the 96,225 points for which $m=33$. The red line is the polygon defined by the 180 points in the Cartesian coordinates obtained from φ_k, ρ_{mk}, where $m=33$ and $k=1,\ldots$, 180 (see the text for the meaning of φ_k, ρ_{mk}) in the case of a Fourier approximation on the order 15. **d** An example with *nSlices* = 50 and *nAngles* = 180. Green dots correspond to the projection on the XY plane of the 96,225 points for which $m=33$. The red line is the polygon defined by the 180 points in Cartesian coordinates obtained from φ_k, ρ_{mk}, where $m=33$ and $k=1,\ldots$, 180 (see the text for the meaning of φ_k, ρ_{mk}) in the case of a Fourier approximation on the order of 25

A different mesh, in which only the areas that contain points are considered, can be built by following an extremely similar procedure. This requires recording the positions m, k for which the values of ρ_{mk} are true and not interpolated, and building a triangle only when all three vertices are among these values.

The final mesh is exported to the 3DReshaper program, where some dimensional features are parameterised.

With the exception of the cited CGAL-free routines (used in the final remeshing), the software program used in the mesh building process was
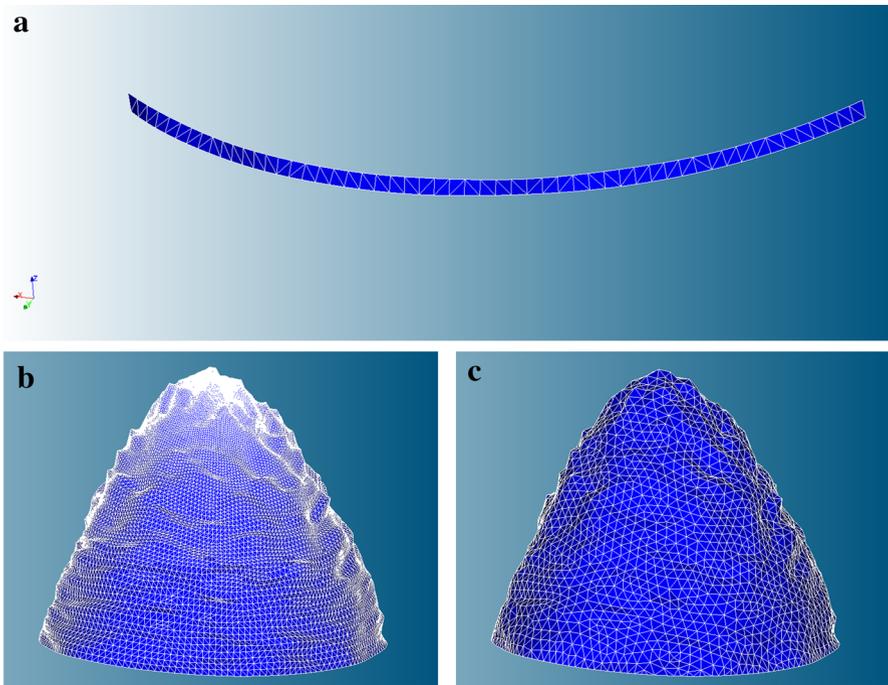
Fig. 5 **a** Details of a piece of triangular mesh between two polygons obtained by splitting the rectangles. **b** Example of one full triangular mesh. **c** Example of one full triangular mesh after remeshing

developed and implemented by the authors. This software was specifically intended for this specific study. The authors plan to use variations of this program for other similar studies in the future. Commercial software used in this study include 3DReshaper (used for post processing) and auxiliary software such as Salome-Meca (used to visualise the meshes, as shown in Fig. 5a–c) and gnuplot (used to represent some of the intermediate files, as indicated in Fig. 4a–d).

Results

The developed method allows us to clean and simplify the point cloud obtained using photogrammetry and to obtain a complete mesh without holes. The characteristics of the survey—the number of photographs used; number of point clouds allowed through the SFM; number of point clouds allowed through the developed program; area of the mesh; dome volume, height, and perimeter; and dimensional parameters—are listed in Table 2. The first five columns list the results and the simplifications developed for the analysis. The last three columns list the dimensional characteristics of the dome obtained using 3DReshaper.

Table 2 Characteristics of the point clouds and mesh

COCONS	Number of photographs	Number of point clouds (SFM)	Number of point clouds (developed program)	Number of triangles (developed program)	Area of the mesh (m²)	Volume (m³)	Height (m)	Perimeter (m)
Cocó 1	28	1,120,931	1249	2316	7.94	2.620	1.42	6.440
Cocó 2	39	3,322,307	3658	7134	8.63	2.905	1.47	6.927
Cocó 3	39	2,396,514	2015	2848	13.50	5.240	2.18	7.974
Cocó 4	29	3,477,150	2521	4860	17.35	8.290	2.43	9.596
Cocó 5	117	4,820,003	4404	8626	9.91	3.504	1.23	9.082
Cocó 6	92	6,338,801	1884	3586	12.70	4.396	1.89	9.038
Cocó 7	75	5,145,146	1795	3408	11.95	4.991	1.49	8.632
Cocó 8	73	6,460,689	1719	3256	11.27	4.500	1.06	8.064
Cocó 9	109	7,917,751	2292	4402	15.81	7.455	1.37	9.723
Cocó 10	64	5,040,074	863	1544	5.16	1.308	0.91	6.165

The number of photographs range between 28 and 109. The number of resulting point clouds (from Photoscan) have a proportional relation with the number of photographs, the range of which is 1,120,931–7,917,751.

The next point cloud is the result of applying the processes of the developed program with a reduction of 1/1000 points. Therefore, the number of points used to generate a realistic mesh when using our software is less than that using the SFM. If a correlation study between the number of point clouds of all cocons and the number of point clouds obtained through the program developed is made, the relation between the initial point cloud and the final version has a correlation of 0.0014. This is due to the applied method eliminating the unessential points to obtain a complete mesh of the domes. The generation of triangles has a proportional relation with the last point cloud in all cocons (Fig. 6).

In the dimensional data, we observe that the perimeter and the height have a poor relation, with a linear regression of 0.192. The last data indicate that the plan is irrelevant to the development of the section (Figs. 7 and 8). However, the linear regression between the area and volume maintains a strong relation.

Discussion

After the results of the building typology are studied and understood, the method allows the generation of a complete mesh. The irregularities of the stones, lighting conditions, and openings of the buildings are considered, enabling us to obtain the dimensional characteristics of this type of dry-stone construction. The simplified mesh obtained using the photographs of the studio elements allows us to conduct precise studies and begin to extract formal characteristics such as those shown.
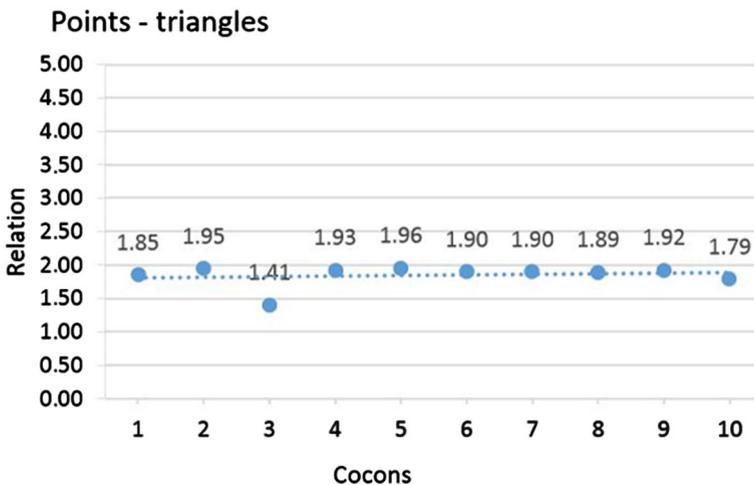
Fig. 6 Linear regression between variable points and triangles (0.9792)

Dispersion graphic of perimeter and height
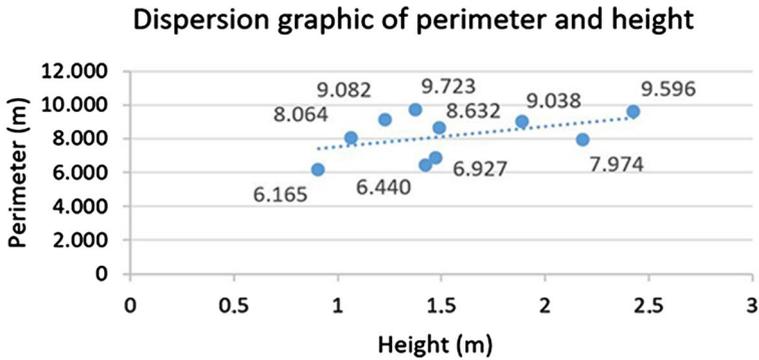
Fig. 7 Linear regression between perimeter and height

Area–volume
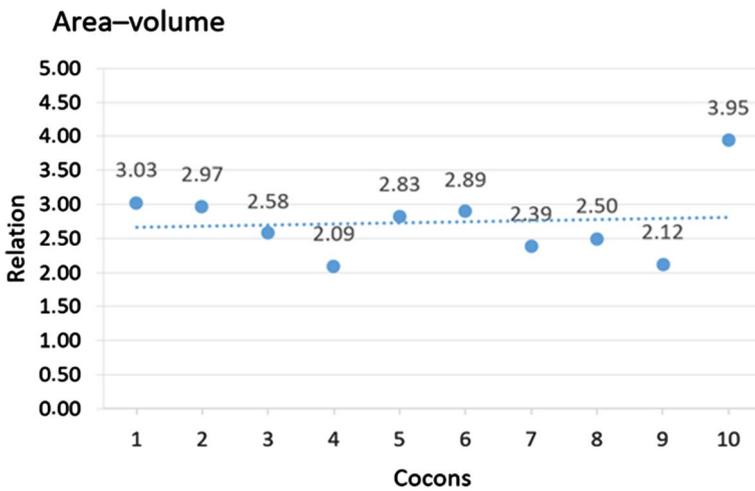
Fig. 8 Correlation between the area and volume (0.96)

The register allows a thorough representation and analysis of the elements of dry stone. Note that light is extremely important to the inner register. Greater illumination means more points because the amount of light is proportional to the number of points. Cocó 10 is a good example to investigate this in greater detail. There are more points obtained to use in the mesh after the SFM is applied because of the ample illumination. This light allows a better definition of the stone.

Conclusions

The method developed in this study is a precise tool for analysing a dry-stone construction in Tivenys. The method used makes it possible to simplify the number of points obtained through photogrammetry, and at the same time complete the cloud of points as precisely as possible.

Being able to automate the cleaning process of the obtained data implies a reduction in the time used to obtain and process the mesh. With the main analysis of the geometric characteristics of dry-stone constructions, the applied methodology allows high precision results to be obtained from incomplete three-dimensional volumes. This methodology, specifically as a first instance for dry stone domes, is applicable to all dry stone constructions built with domes or vaults and even to other heritage buildings, and particularly for constructions with numerous reliefs. This versatility is due to the different phases that make up the methodology, which have been designed using the power methodology of different geometries.

This study marks the beginning of further investigations that will focus on a simplification of the inner and outer faces as a comparative study between the interior and exterior of the cocons. The method will allow us to obtain the thickness of the dome and to complete the characteristics of the construction.

References

Andreu, Javier, Pablo Serrano. 2019. Contributions of the digital photogrammetry and 3D modelling of Roman inscriptions to the reading of damaged tituli: An example from the Hispania Tarraconensis (Castiliscar, Saragossa). *Digital Applications in Archaeology and Cultural Heritage*. https://doi.org/10.1016/j.daach.2019.e00091

Barber, David, Jon Mills, Clive Boardman, Paul Bryan. 2018. Laser Scanning Technology. In *3D Laser Scanning for Heritage: Advice and Guidance on the Use of Laser Scanning in Archaeology and Architecture*, ed. Historic England, 4–24. © APR Services

Botsch, Mario, Leif Kobbelt. 2004. A remeshing approach to multiresolution modeling, *Eurographics/ACM SIGGRAPH symposium on Geometry processing*. https://doi.org/10.1145/1057432.1057457

Botsch, Mario, Leif Kobbelt, Mark Pauly, Pierre Alliez, Bruno Lévy. 2010. *Polygon mesh processing*. CRC Press.

Carnimeo, Leonarda, Dora Foti, Salvador Ivorra. 2015. On Modeling an Innovative Monitoring Network for Protecting and Managing Cultural Heritage from Risk Events. *Key Engineering Materials KEM* 628, 243–249. 10.4028/www.scientific.net/KEM.628.243

CGAL, The Computational Geometry Algorithms Library. n.d. https://www.cgal.org. Accessed 25 May 2019

Chen, Jieh-Haur, M-Chun Su, Ruijun Cao, Shu-Chien Hsu, Jin-Chun Lu. 2017. A self organizing map optimization based image recognition and processing model for bridge crack inspection. *Automation in Construction* 73: 58-66. https://doi.org/10.1016/j.autcon.2016.08.033

Forlin, Paolo, Riccardo Valente, Miklós Kázmér. 2018. Assessing earthquake effects on archaeological sites using photogrammetry and 3D model analysis. *Digital Applications in Archaeology and Cultural Heritage* 9. https://doi.org/10.1016/j.daach.2018.e00073

Foti, Dora, Vitantonio Vacca, Ivana Facchini. 2018. DEM modeling and experimental analysis of the static behavior of a dry-joints masonry cross vaults. *Construction and Building Materials* 170: 111-120.

Fryskowska, Anna, Julita Stachelek. 2018. A no-reference method of geometric content quality analysis of 3D models generated from laser scanning point clouds for hBIM. *Journal of Cultural Heritage* 34 : 95-108. https://doi.org/10.1016/j.culher.2018.04.003

Galantucci, Rosella, Fabio Fatiguso. 2019. Advanced damage detection techniques in historical buildings using digital photogrammetry and 3D surface anlysis. *Journal of Cultural Heritage* 36: 51-62. https://doi.org/10.1016/j.culher.2018.09.014

García, Miguel, Arturo Zaragozá. 2000. *Arquitectura Rural primitiva en secà*. València: Generalitat Valenciana.

Guarnieri, Alberto, Antonio Vettore, Fabio Remondino. 2004. Photogrammetry and Ground-based Laser Scanning: Assessment of Metric Accuracy of the 3D Model of Pozzoveggiani Church. *Féderation Internationale des Géomètres Working Week*

Jalandoni, Andrea, Inés Domingo, Paul Tacon. 2018. Testing the value of low-cost Structure-from-Motion (SfM) photogrammetry for metric and visual analysis of rock art. *Journal of Archaeological Science* 17: 605-616. https://doi.org/10.1016/j.jasrep.2017.12.020

Koutsoudis, Anestis, Blaz Vidmar, George Ioannakis, Fotis Arnaoutoglou, George Pavlidis, Christodoulos Chamzas. 2014. Multi-image 3D reconstruction data evaluation. *Journal of Cultural Heritage* 15(1): 73-79. https://doi.org/10.1016/j.culher.2012.12.003

Leserri, Massimo, Gabriele Rossi. 2013. Arquitecturas de piedra seca, un levantamiento problemático. *Expresión Gráfica Arquitectónica* 22: 184-195. https://doi.org/10.4995/ega.2013.1532

Lluch, Ernest, Eugeni Giralt. 1967. *L'economia de la regió de l'Ebre*. Bacelona: Servei d'Estudis de la Banca Catalana.

Mecca, Saverio, Letizia Dipasquale. 2009. *Earthen domes and habitats. Villages of Northern Syria.* Pisa: EDIZIONI ETS.

Mineo, Carmelo, Stephen Gareth, Rahul Summan. 2019. Novel algorithms for 3D surface point cloud boundary detection and edge reconstruction. *Journal of Computational Design and Engineering* 6(1): 81-91. https://doi.org/10.1016/j.jcde.2018.02.001

Pavlidis, George, Anestis Koutsoudis, Fotis Arnaoutoglu, Vassilios Tsioukas, and Christodoulos Chamzas. 2007. Methods for 3D digitization of Cultural Heritage. *Journal of Cultural Heritage* 8: 93–98.

Restuccia, Franca, Corrado Fianchino, Mariateresa Galizia, Cettina Santagati. 2012. The stone landscape of the Hyblaen Mountains: the geometry, structure, shape and the muragghio. *Domes in the World. Congress Proceedings*: 1–14. ISBN 978884044211

Rubió, Joan. 1914. Construccions de pedra en sec. In *Anuario de la Asociación de Arquitectos de Cataluña*. Barcelona: Collegi d'Arquitectes de Barcelona.

Tarragó, Salvador. 2006. *Actes del 1r. Col·loqui Internacional de construcció de pedra seca*. Barcelona: Aguazul.

Todisco, Leonardo, Giuseppe Sanitate, Giuseppe Lacorte. 2017. Geometry and Proportions of the Traditional Trulli of Alberobello. *Nexus Network Journal* 19: 701-721. https://doi.org/10.1007/s00004-016-0326-4

Torres, Leopoldo. 1933. *La vivienda popular en Españ*a. Barcelona: A. Martín.

Vegas, Fernando, Camilla Mileto, Valentina Cristini. 2010. Corbelling domes and bridges in Spain and Portugal: a comparative study. *ARCH'10- 6th International Conference on Arch Bridges*: 298–303

Venerito, Marilena, Dora Foti, Michele Vitti. 2017. On the static and dynamic behavior of a prehistoric structure typical of Apulia in Italy. *Procedia Engineering* 180: 480-490. https://doi.org/10.1016/j.proeng.2017.04.207

Cèlia Mallafrè Balsells is an architect with a degree from the Reus School of Architecture (ETSA) of the Rovira i Virgili University (URV), with a specialization in Architectural Heritage. Currently she is a PhD student in the Rovira i Virgili University (URV) and "El Solà" Foundation (The Industrial Doctorates

Plan of Generalitat de Catalunya). Her research focuses on architectural heritage, with a special focus on dry-stone technique and constructions.

Josep Maria López is titular professor of Rovira i Virgili University (URV) in the department of Computer Engineering and Mathematics. His research focuses on Applied Mathematics.

Agustí Costa Jover is an architect with a degree from the Barcelona School of Architecture (ETSAB) of the Polytechnic University of Catalunya (UPC), Master in "Technology of Architecture. Restoration and Rehabilitation", and PhD from the Rovira i Virgili University (URV). Currently he is Serra Hunter Fellow at the Reus School of Architecture (ETSA) of the URV. His research is focused on construction history and architectural heritage, with a special focus on the use of massive data capture techniques for the study of historical constructions.

Sergio Coll Pla is an architect with a degree from the Barcelona School of Architecture (ETSAB) of the Polytechnic University of Catalunya (UPC) and a PhD by the Rovira i Virgili University (URV). Currently he is research professor at the Reus School of Architecture (ETSA) of the URV. His research is focused on construction history, architectural heritage and energetic characteristics of the heritage.